ISSN: 2148-9173 **Vol: 8 Issue:4 December 2021**

International Journal of Environment and Geoinformatics (IJEGEO) is an international, multidisciplinary, peer reviewed, open access journal.

Determination of forest burn scar and burn severity from free satellite images: a comparative evaluation of spectral indices and machine learning classifiers

Nooshin MASSHADI, Ugur ALGANCI

Abstracting and Indexing: TR DIZIN, DOAJ, Index Copernicus, OAJI, Scientific Indexing Services, International Scientific Indexing, Journal Factor, Google Scholar, Ulrich's Periodicals Directory, WorldCat, DRJI, ResearchBib, SOBIAD

International Journal of Environment and Geoinformatics 8(4):488-497 (2021)

Reaserch Article

Determination of forest burn scar and burn severity from free satellite images: a comparative evaluation of spectral indices and machine learning classifiers

Nooshin Masshadi[1], Ugur Alganci[2,*]

[1] Istanbul Technical University, Graduate School, Geographical Information Technologies Programme, Istanbul, Turkey
[2] Istanbul Technical University, Civil Engineering Faculty, Geomatics Engineering Department, Istanbul, Turkey

* Corresponding author: U. Alganci
E-mail: alganci@itu.edu.tr

Received 13.02.2021
Accepted 22.08.2021

How to cite: Masshadi and Alganci (2021). Determination of forest burn scar and burn severity from free satellite images: a comparative evaluation of spectral indices and machine learning classifiers, *International Journal of Environment and Geoinformatics (IJEGEO)*, 8(4):488-497. doi.10.30897/ijegeo.879669

Abstract

Remote sensing data indicates a considerable ability to map post-forest fire destructed areas and burned severity. In this research, the ability of spectral indices, which are difference Normalized Burned Ratio (dNBR), relative differenced Normalized Burn Ratio (RdNBR), Relativized Burn Ratio (RBR), and difference Normalized Vegetation Index (dNDVI), in mapping burn severity was investigated. The research was conducted with free access moderate to high-resolution Landsat 8 and Sentinel 2 satellite images for two forest fires cases that occurred in Izmir and Antalya provinces of Turkey. Performance of the burn severity maps from different indices were validated by use of NASA Firms active fires dataset. The results confirmed that, RdNBR showed more precise results than the other indices with an accuracy of (89%, 93%) and (84%, 79%) for Landsat 8 and Sentinel 2 satellites over Izmir and Antalya respectively. Moreover, in this research, the ability of machine learning classifiers, which are Support Vector Machine (SVM) and Random Forest (RF), in mapping burned areas were evaluated. According to the accuracy metrics that are user's accuracy, producer's accuracy and Kappa coefficient, we concluded that both classifiers indicate reliable and accurate detection for both regions.

Keywords: Forest fire, Burn scar, Burn severity, Landsat 8, Sentinel 2

Introduction

Forest fire is a pivotal ecological disaster in many forested areas, and the level of its severity noticeably affects forest management and wildlife habitat (Herrando and Brotons 2002; Herrando et al. 2003; Burak et al., 2004; Erten et al., 2004; Özcan et al., 2018). Although there are numbers of forest disturbances that affect the ecosystem, fire-induced changes are mentioned to be the most destructive one (Seidl et al. 2017).

Most of the remote sensing-based burn scar and burn severity detection studies rely on the unique spectral response and changes in these responses after the fire occurrence over the affected areas. The previous detection studies were performed either with bi-temporal or after fire satellite images (Miller and Thode 2007; Parks et al. 2014; Evangelides and Nobajas 2020; Gibson et al. 2020). Previous researches proved that, spectral indices are powerful in burned area monitoring (Chuvieco et al. 2002; Miller and Thode 2007; Mouillot et al. 2014). Thematic information extraction and boundary delineation requirements are mostly fulfilled by the use of threshold-based clustering or classification approaches.

One of the most effective and common ways to obtain burn severity maps (Soverel et al. 2010; Fernández-García et al. 2018) and assessment of damaged areas, is threshold-based clustering of spectral indices, especially the ones that use NIR and SWIR spectral regions (Lutes et al. 2006). As an example, differenced Normalized Burn Ratio (dNBR) seeks for decrease in near infrared (NIR) region and an increase in shortwave infrared (SWIR) region in the post-fire image analysis scenario (Mallinis et al. 2018). In addition, the classification approaches for detection is mostly performed in a supervised manner, by feeding the algorithms with spectral /index characteristics of the identifiable sample regions. In the last decade, there is a general trend of using pixel-based machine learning algorithms or object-based image analysis (OBIA) classification approaches (Sertel and Alganci, 2016).

On the data side, the free accessibility of Landsat-8 and Sentinel-2 images opens a new era for medium resolution global land surface monitoring (Drusch et al. 2012; Roy et al. 2014). It is proved that Landsat data can map small and spatially fragmented burned areas that are not visible in coarser spatial resolutions (Scholes et al. 1996; Laris 2005; Silva et al. 2005). Additionally, studies have shown the suitability and even superiority of Sentinel-2 data in natural resources applications (van der Werff and van der Meer 2016; Shoko and Mutanga 2017). The effectiveness of Sentinel-2 twin satellites to detect burned areas and reforestation with accuracy improvement have been demonstrated in several studies (Huang et al. 2016; Navarro et al. 2017; Rahman et al. 2019).

Supervised classification of remote sensing data through machine learning approaches such as random forest (RF) and support vector machine (SVM) have been widely used in the context of burned forest areas to calculate the precise amount of burned areas, which plays a prominent role for managing forest cover landscapes (Cutler et al. 2007; Rodriguez-Galiano et al. 2012; Collins et al. 2018). With the inspiration from current advances in satellite missions and analysis strategies for satellite image-based forest fire detection and burn severity mapping, this research mainly focused on a comparative evaluation of detection accuracies with different satellite, spectral index and classification algorithm configurations.

The objective of the research can be considered two-fold, first to evaluate the accuracy of fire severity classification from spectral indices such as differenced Normalized Burn Ratio (dNBR), Relativized Burn Ratio (RBR), and Relative differenced Normalized Burn Ratio (RdNBR) that obtained from Landsat 8 and Sentinel-2 satellite images. The second objective is to evaluate the efficiency of machine learning-based supervised classifiers in burned area detection by taking the SVM and RF algorithms as the candidates.

Study Area

The forest fires in Izmir and Antalya regions that occurred in August 2019 and June 2016 respectively were selected as the case fires of this research. The Turkish General of Directorate of Forestry delineated that the total forest area of the Izmir province is 475,779 ha and 146 forest fires occurred in 2019 (RTGDF, 2019). One of these forest fires occurred on the 18th August 2019 in Gaziemir, Buca, and Karabağlar districts of Izmir, and approximately 5,000 ha of forest areas were affected (Kesgin Atak and Ersoy Tonyalioglu, 2020). For the second case, the forest fire that occurred on 24-27 June 2016 in Adrasan and Kumluca regions of Antalya province were investigated. The province of Antalya is located in the Mediterranean climate zone, where there is a risk of first-degree fire. The existing forest area is 1,146,062 ha, covering 56% of the province's surface area and correspond to 5.4% of the forest areas of Turkey. The regions of interest for this research are provided in Figure 1.

Materials and Methods
Data

The Sentinel 2 and Landsat 8 satellite images for post-fire and pre-fire dates were downloaded from the Earth Explorer archive. Images were selected from the available cloud-free pre- and post-fire archives that were closest to the date of the fire, aiming to avoid phenological changes in the vegetation and to allow comparison among remote sensing products in estimating burn severity (García-Llamas et al. 2019), (Table1).

The active fire point dataset was downloaded from FIRMS NASA website and used to validate the burn severity maps and burned area detection results derived from Landsat 8 and Sentinel 2 images (Konkathi and Shetty 2019; Bar et al. 2020). This dataset is produced from Moderate Resolution Imaging Spectro-radiometer (MODIS) and SUOMI NPP Visible Infrared Imaging Radiometer Suite (VIIRS) images and distributed with confidence information. The fire points were taken from 18th August 2019 to 20th August 2019 for Izmir and were taken from 24th June 2016 to 26th June 2016 for Antalya.

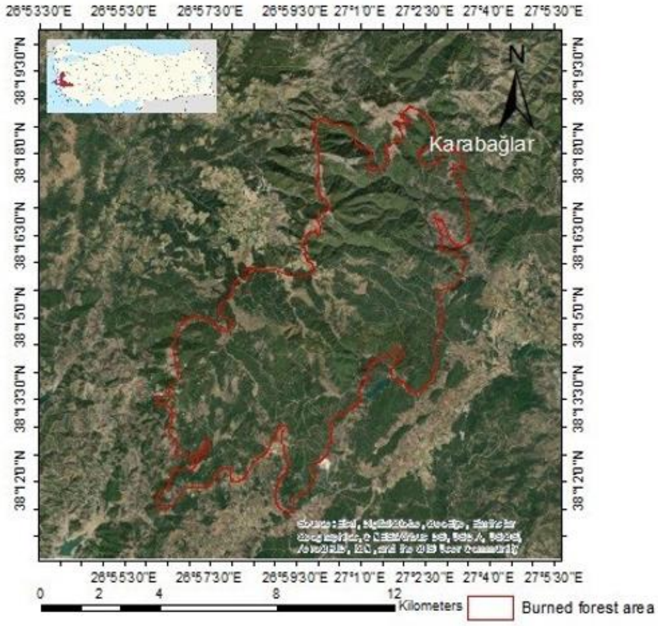

(a)

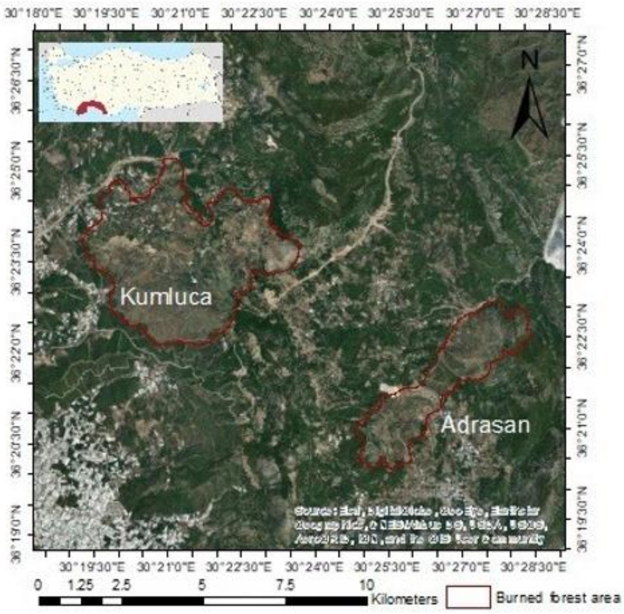

(b)

Fig. 1. The study area (a) Karabağlar, Izmir (b) Adrasan and Kumluca regions, Antalya

Table 1. Satellite images information and date of acquisition

Study site	Dataset	Resolution	Acquisition dates (Pre / post Fire)
Izmir	Landsat 8	30m	07.08.2019 / 23.08.2019
	Sentinel 2	10m, 20m	11.08.2019 / 21.08.2019
Antalya	Landsat 8	30m	22.06.2016 / 08.07.2016
	Sentinel 2	10m, 20m	21.06.2016 / 11.07.2016

Preprocessing

The processing chain of this research is provided in Figure 2. As a first step, Sentinel-2 data were atmospherically corrected in SNAP (Zuhlke 2015) using the sen2cor tool (Louis et al. 2016). Landsat 8 data were atmospherically corrected in ENVI© software using the Fast Line-of-sight Atmospheric Analysis of Hypercubes (FLAASH) algortihm. The Sentinel 2A and Landsat 8 OLI images are provided as geometrically corrected, thus, no geometric correction was performed (Sothe et al., 2017). For Sentinel 2 data, bands 11 and 12 with 20m resolution were resampled to 10m resolution in SNAP. After Layer stacking, bands of the selected Landsat-8 and Sentinel-2A images were standardized using the following formula (Rahman, et al., 2019):

$$(Bi \leq 0) \times 0 + (Bi \geq 10000) \times 1 + (Bi \geq 0 \text{ and } Bi < 10000) \times \text{float}(Bi)/10000 \quad (1)$$

where, Bi = Specific Band

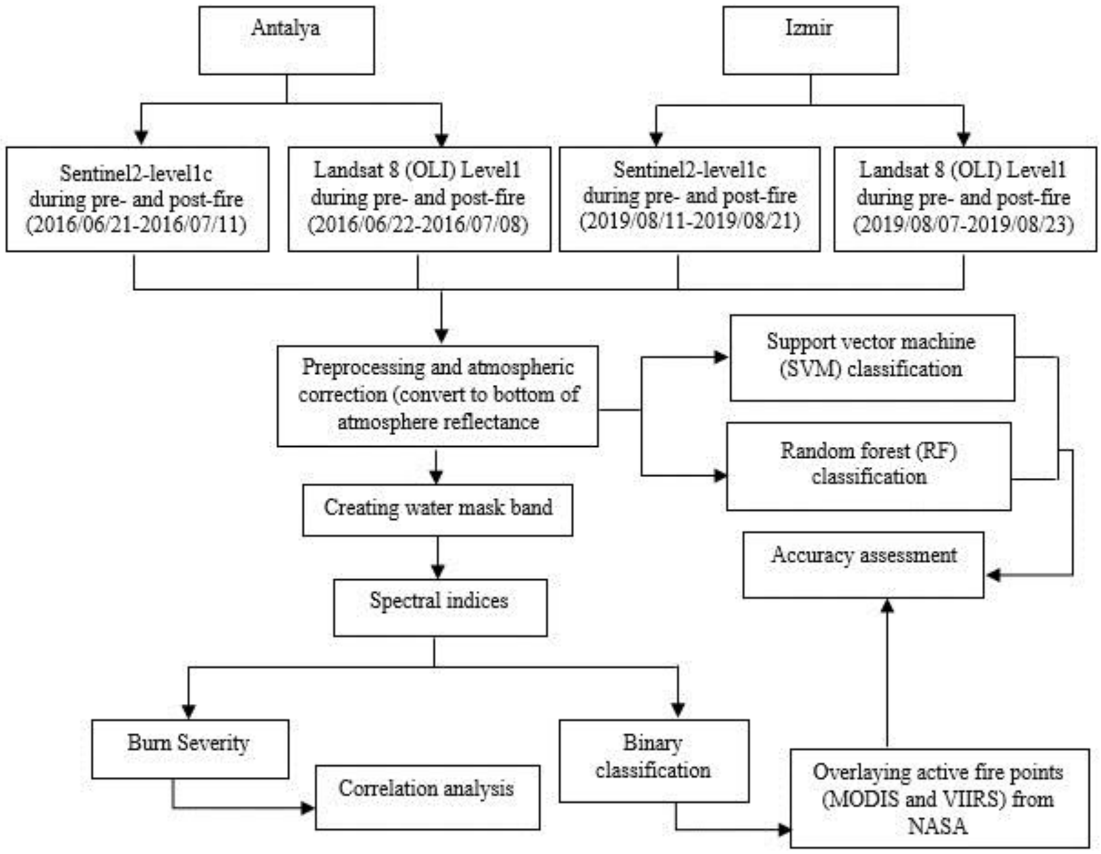

Fig. 2. Methodological flowchart.

Spectral Index Calculation and Burn Severity Mapping

Burn severity is a measure for evaluating the magnitude of ecological alteration caused by a forest fire. This research evaluates the performance of four spectral indices that are dNDVI, dNBR, RdNBR, and RBR in burn severity detection and mapping. For this purpose, a series of bi-temporal spectral indices were calculated from satellite images (Mallinis, et al., 2018). Normalized difference vegetation index (NDVI) is the most popular vegetation index, as it provides a measure of vegetation greenness and photosynthetic activity (Fraser, et al., 2000). The NBR is specifically designed to extract the burned areas and determine burn severity. It uses the NIR and SWIR bands, which are different from the NDVI (Red and NIR bands) in the calculation. The NBR is also crucial for determining, measuring, and mapping burn severity quantitatively and qualitatively (Key and Benson, 2005). Post-fire NBR is subtracted from pre-fire NBR to provide dNBR for assessing burn severity. NBR index values theoretically vary from –1 to + 1, whereas dNBR values can vary from – 2 to + 2. Relative difference Normalized Burn ratio (RdNBR) was a variant of the Differenced Normalized Burn Ratio (dNBR) that considers the relative amount of pre-to post-fire change by dividing dNBR by the pre-fire NBR value This index was proposed to remove the bias due to the pre-fire vegetation type and density (Miller, et al., 2009).

The list of all indices used in this study for each satellite has been shown in Table 2. The burn severity indices values were classified into different severity levels according to the burn severity category indicated by the US Geological Survey (USGS, 2016) (Table 3).

Table 2. Spectral indices for Landsat 8 and Sentinel 2 satellites

Spectral index	Sentinel2	Landsat8	References
Normalized Difference Vegetation Index (NDVI)	$NDVI=\frac{(Band8-Band4)}{(Band8+Band4)}$	$NDVI=\frac{(Band5-Band4)}{(Band5+Band4)}$	Tucker, 1979
Normalized Burn Ratio (NBR)	$NBR=\frac{(Band8-Band12)}{(Band8+Band12)}$	$NBR=\frac{(Band5-Band7)}{(Band5+Band7)}$	Key and Benson, 2005
Difference normalized vegetation index (dNDVI)	$dNDVI=NDVI_{pre-fire}-NDVI_{post-fire}$	$dNDVI=NDVI_{pre-fire}-NDVI_{post-fire}$	
differenced Normalized Burn Ratio (dNBR)	$dNBR=NBR_{pre-fire}-NBR_{post-fire}$	$dNBR=NBR_{pre-fire}-NBR_{post-fire}$	Key and Benson, 2005
Relativized Burn Ratio (RBR)	$RBR=\frac{dNBR}{(NBR_{pre-fire}+1.001)}$	$RBR=\frac{dNBR}{(NBR_{pre-fire}+1.001)}$	Parks, Dillon and Miller, 2014
Relative differenced Normalized Burn Ratio (RdNBR)	$RdNBR=\frac{dNBR}{(abs(NBR_{pre-fire}/1000))^{0.5}}$	$RdNBR=\frac{dNBR}{(abs(NBR_{pre-fire}/1000))^{0.5}}$	Miller et al., 2009

Table 3. Severity category definitions (©USGS)

Range	Burn severity
< – 0.25	High post-fire regrowth
– 0.25 to – 0.1	Low post-fire regrowth
– 0.1 to + 0.1	Unburned
0.1 to 0.27	Low-severity
0.27 to 0.44	Moderate-low severity
0.44 to 0.66	Moderate-high severity
>0.66	High-severity

Burned Area Detection with Classification

According to the objective of this study, post-fire supervised classification of Sentinel 2A and Landsat 8 OLI satellites for both study areas were performed by the use of pixel-based machine learning algorithms that are Support Vector Machine (SVM) and Random Forest (RF). Support Vector Machines are an efficient statistical classification method that determines how to define the boundary line (hyperplane) that can best distinguish two or more classes from each other (Huang et.al., 2002). The RF algorithm generates an ensemble of regression trees, through a bootstrap aggregated (bagging) sampling of training data (Breiman, 2001). At each node in a decision tree, a random selection (parameter entry) of predictor variables is evaluated for their ability to split training data into response classes, with the variable leading to the most homogeneous classification being selected.

In this research, a stratified random training sample dataset was created for classification, based on the number of classes for each study area. For making a comparison between SVM and RF classification algorithms, the same training samples were used for each of the algorithms according to the number of classes for the study areas (Izmir and Antalya). The open-access software QGIS 3.10, classification tool (dzetsaka) plugin was used for process.

Accuracy Assessment

Point data for burned and unburned areas were used to test classification algorithms. The test points for unburned areas were randomly generated and assigned to each class by using the satellite image as the base map. The burned areas were tested using NASA FIRMS active fire point data. As this dataset is generated from MODIS and VIIRS images that have coarse spatial resolution, it faces difficulties in detecting the spatial extent of smaller fires. The main limitation of such a technique is the low spatial accuracy of the hotspot detections that causes false correspondences between vegetation changes and active fires (Roteta, et al., 2019). Considering these limitation, only the fire points with a confidence level higher than 90% were used for both regions. A set of accuracy assessment metrics such as User Accuracy (UA), Producer Accuracy (PA), Kappa (K) and Overall Accuracy (OA) were used for the assessment (Foody, 2010).

Results and Discussion

According to the initial aim of this research, spectral indices dataset classified into different severity levels based on burn severity categories provided by USGS to produce burn severity maps for each study area (Fig. 3). To evaluate the accuracy of these maps produced from different indices, active fire points from NASA FIRMS were overlaid on binary classified (burned vs unburned) burn severity maps. The overall accuracy results and the amount of burned area derived from different indices and for each satellite were graphed in Figure 4. In general, without considering dNDVI data set, the Sentinel 2 image-based analysis provided higher accuracy than the analysis with Landsat 8 dataset in Karabağlar, Izmir. Besides, RdNBR represented a high level of accuracy for both S_2 and L_8 satellites, 93% and 89% respectively. In Kumluca and Adrasan, Antalya, dNDVI and RdNBR L_8 showed the same accuracy of 84%. However, in S_2 both dNBR and RdNBR represented 79% overall accuracy. Thus, the relativized RdNBR index, which provides information on the changes induced by fire regardless of pre-fire land cover (Miller and Thode, 2007), may more accurately predict burn severity in heterogeneous landscapes (Miller, et al., 2009). Moreover, the burned area analysis provided different values for satellites and bi-temporal indices. The dNDVI with L_8 provided a higher burned area than S_2 over Karabağlar, Izmir, whereas other indices represented a higher amount of burned area with S_2 satellite images for this region. Besides, the same result can be observed in Adrasan and Kumluca regions, Antalya. Classification results from two machine-learning algorithms for both satellites over the study areas were given in Figure 5

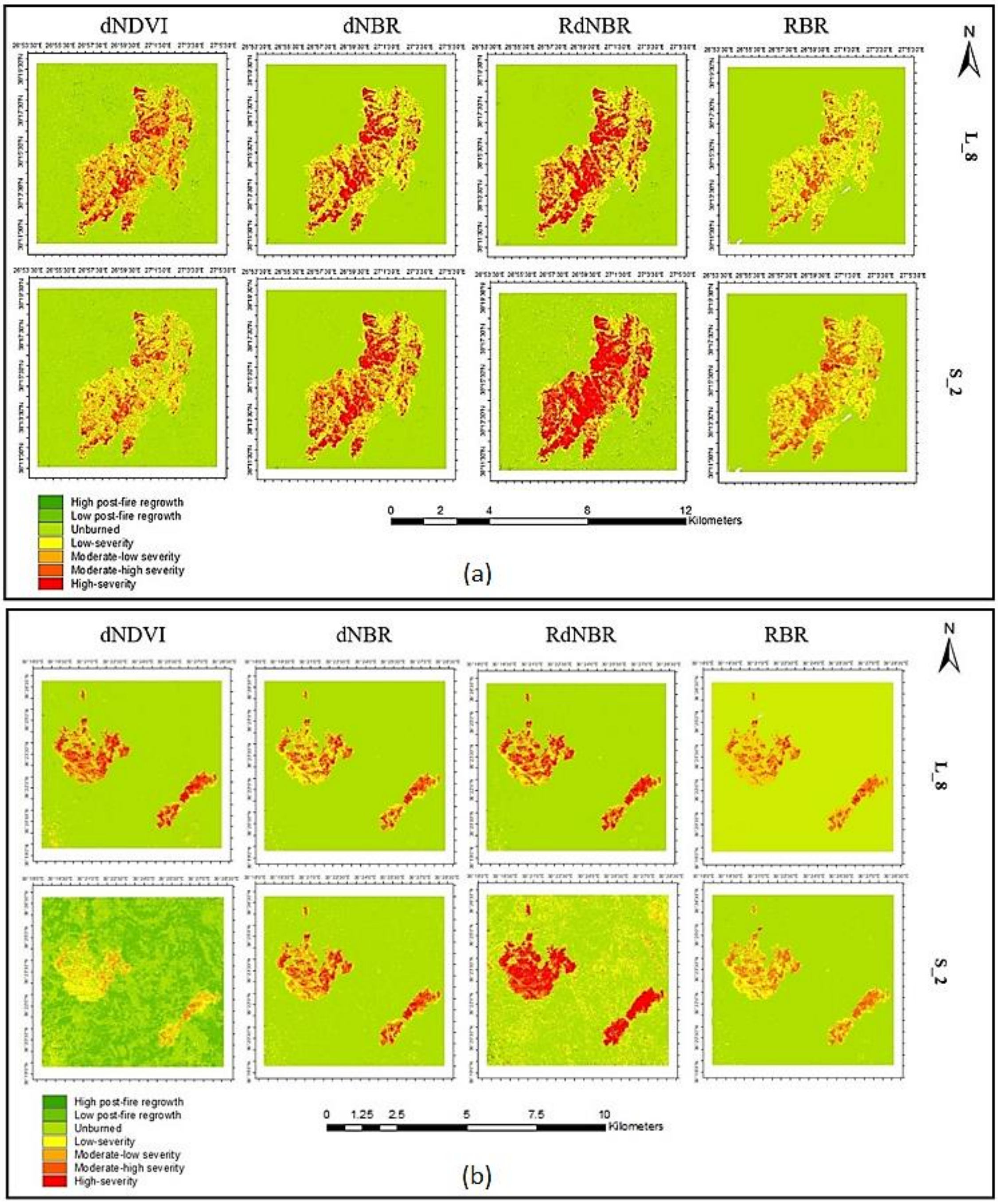

Fig. 3. Severity maps of indices for Landsat 8 (L_8) and Sentinel 2 (S_2) (a) Karabağlar, Izmir (b) Adrasan and Kumluca regions, Antalya

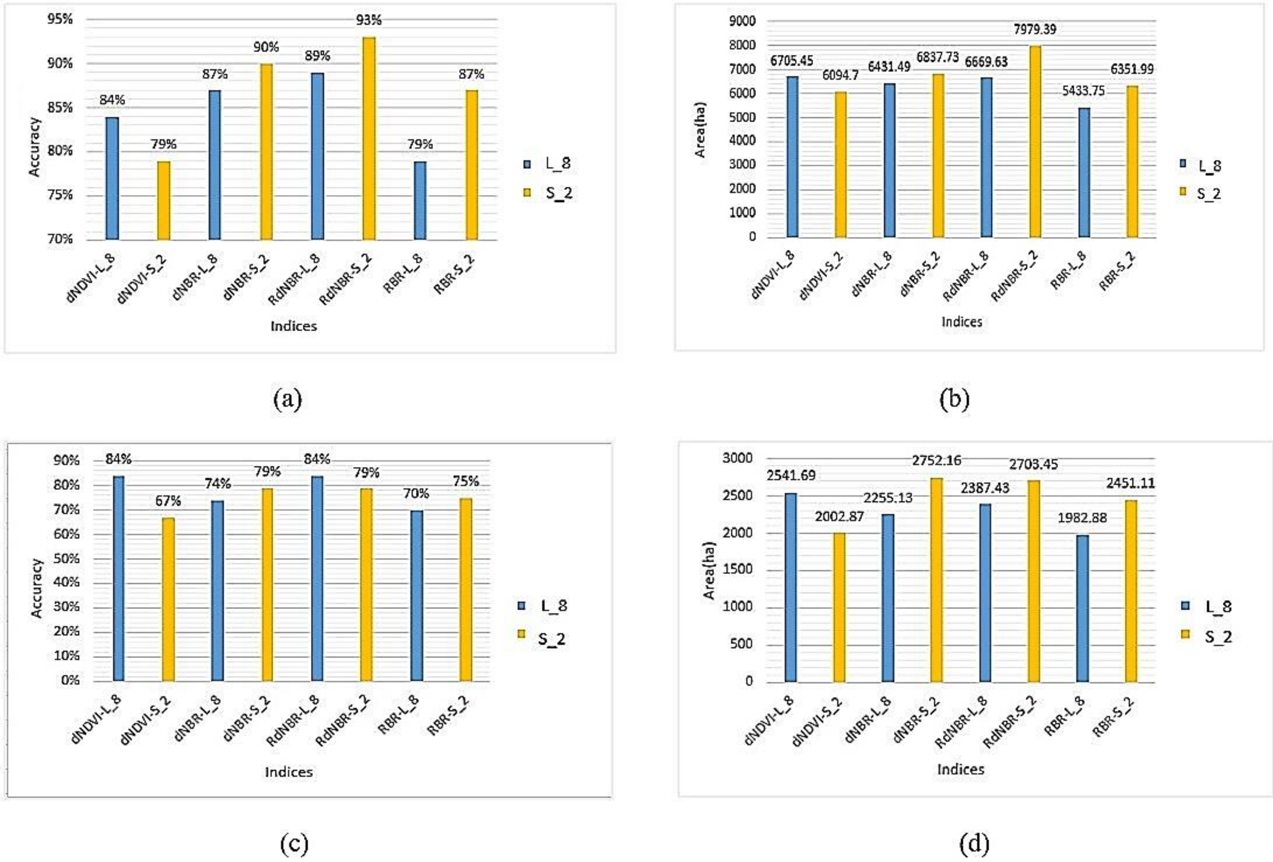

Fig. 4. Landsat 8 OLI (L_8) and Sentinel 2 (S_2) overall accuracy and total burned area (ha) derived from binary classification of severity indices over Karabağlar, Izmir (a), (b) and Adrasan and Kumluca regions, Antalya (c), (d).

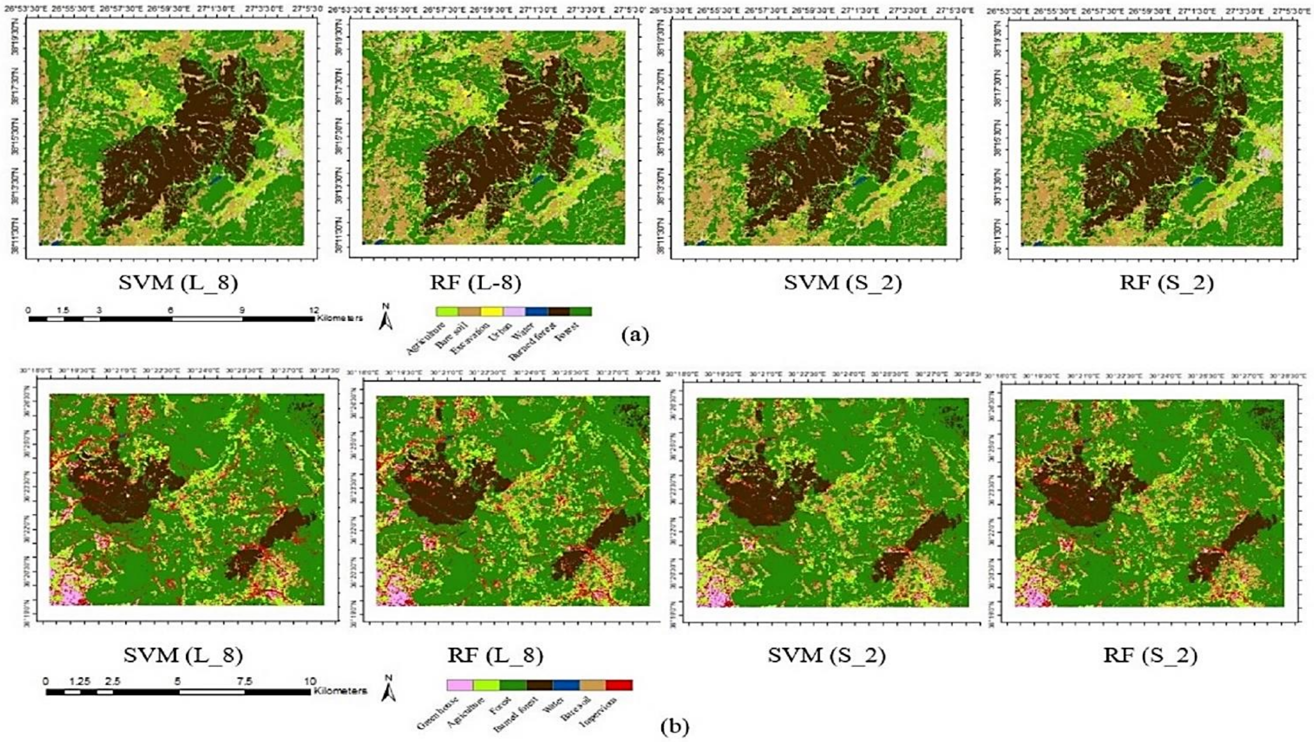

Fig. 5. ML classifications derived from Landsat 8 (L_8) and Sentinel 2 (S_2) over the study areas (a) Karabağlar, Izmir and (b) Adrasan and Kumluca, Antalya

A comparison of burned area estimation between two ML classifiers (SVM and RF), over the two study areas by using the post-fire images derived from L_8 and S_2 is represented in Table 4. According to this table, the RF classifier provided a higher amount of burnt area than the SVM classifier in Adrasan and Kumluca, Antalya for both satellites. Moreover, in this area with respect to relative difference L_8 approximately represented similar results, however, S_2 showed a 4.5% difference for different classifiers. In Karabağlar, Izmir SVM classifiers indicated more amount of burned areas in comparison with RF. Moreover, the amount of burned areas derived from SVM and RF-based on S_2, more close to each other in comparison with L_8.

Several machine-learning algorithms have been used for burned area assessment, however the RF algorithm was mostly employed widely to identify burnt vegetation (Bar et al., 2020). In this research, two different ML classifiers (i.e. SVM and RF) were applied with the same set of training data over two study areas for both satellites to make a comparison and evaluate the performance of each in burned forestry areas. Producers Accuracy (PA), User Accuracy (UA), Overall Accuracy (OA), and Kappa coefficient were employed to evaluate the performance of these classifiers on different satellite images (Table 5 and Table 6). For the PA scores for the burned areas, the SVM provided slightly higher scores than the RF, and with a slightly better result for the L_8 satellite for both algorithms in the Izmir region. For the Antalya region, the RF provided slightly better scores than the SVM again in favour of the L_8 satellite image. For the UA metric, both algorithms and satellite images provided a 100% score for Izmir, while all the configurations except the RF classification of L_8 image provided efficient scores over 90% for the Antalya region. The OA metric for all configurations provided acceptable performances around 85%. The amount of Kappa coefficient in test regions was varied between 0.8-0.87. Tran et al (2018) claim that kappa values greater than 0.77 represent substantial agreement for the accuracy of burned areas.

Table 4. Burned area estimation over study areas for SVM and RF based on S_2 and L_8 (ha)

	Antalya			Izmir		
Sat.	SVM	RF	diff. (%)	SVM	RF	diff. (%)
L_8	2199.96	2212.38	0.28	5895.63	5722.56	1.50
S_2	2095.20	2294.17	4.50	5863.25	5790.83	0.62

Table 5. Accuracy assessment of ML algorithms on Sentinel 2 and Landsat 8 surface reflectance images for Karabağlar, Izmir

	Sentinel 2				Landsat 8			
	SVM		RF		SVM		RF	
Class name	Producers acc.	Users acc.	Producers acc.	Users acc.	Producers acc.	Users acc.	Producers acc.	Users acc.
Agriculture	80%	81%	80%	80%	86%	77%	84%	82%
Bare soil	82%	77%	88%	78%	76%	82%	70%	72%
Excavation	89%	78%	89%	74%	89%	79%	89%	73%
Urban	73%	79%	69%	92%	75%	77%	77%	77%
Water	100%	100%	100%	100%	100%	100%	100%	100%
Burned forest	78%	100%	76.5%	100%	82%	100%	79.5%	100%
Forest	100%	82%	100%	86%	100%	87%	100%	88%
Overall acc.	89%		86%		84%		85%	
Kappa	0.87		0.85		0.80		0.82	

Table 6. Accuracy assessment of ML algorithms on Sentinel 2 and Landsat 8 surface reflectance images for Adrasan and Kumluca, Antalya

	Sentinel 2				Landsat 8			
	SVM		RF		SVM		RF	
Class name	Producers acc.	Users acc.	Producers acc.	Users acc.	Producers acc.	Users acc.	Producers acc.	Users acc.
Greenhouse	86%	100%	88%	98%	84%	98%	88%	100%
Agriculture	92%	88%	86%	54%	90%	80%	86%	47%
Forest	96%	74%	96%	76%	96%	75%	96%	77%
Burned forest	66%	95%	72%	98%	70%	91%	72%	62%
Water	100%	100%	100%	100%	100%	100%	100%	100%
Bare soil	94%	85%	92%	90%	90%	88%	92%	90%
Impervious	90%	83%	90%	80%	80%	80%	78%	42%
Overall	86.5%		87%		85%		85%	
Kappa	0.84		0.84		0.81		0.82	

The correlation analysis between fire severity metrics (dNDVI, dNBR, RdNBR, and RBR) were calculated to evaluate the level of agreement between these bi-temporal indices and to define the best pairs for fire severity detection. According to the results are provided in Figure 6, for Landsat 8 in Karabağlar, Izmir there is a strong correlation between RBR with dNBR, and RdNBR However there is a with a strong scattering of dNDVI that indicates lower correlation. The high correlation (0.95-0.99) indicates that related indices would be effective to determine forest fire severity. Landsat 8 indicated a similar result over Adrasan and Kumluca, Antalya with a high correlation (0.92-0.99) between these bi-temporal indices. For Sentinel 2 image dataset, the reduced correlation of dNDVI with other indices due to its scattered characteristics becomes more obvious. This finding can be supported by Figure 3b, where dNDVI failed to detect high severity areas. From the sensor aspect, the function lines are in much linear characteristics for Landsat 8, indicating higher similarity between indices, on the other hand Sentinel 2 data related graphs provided non-linear characteristics, which indicate special attention requirement when designing threshold based analysis from these indices.

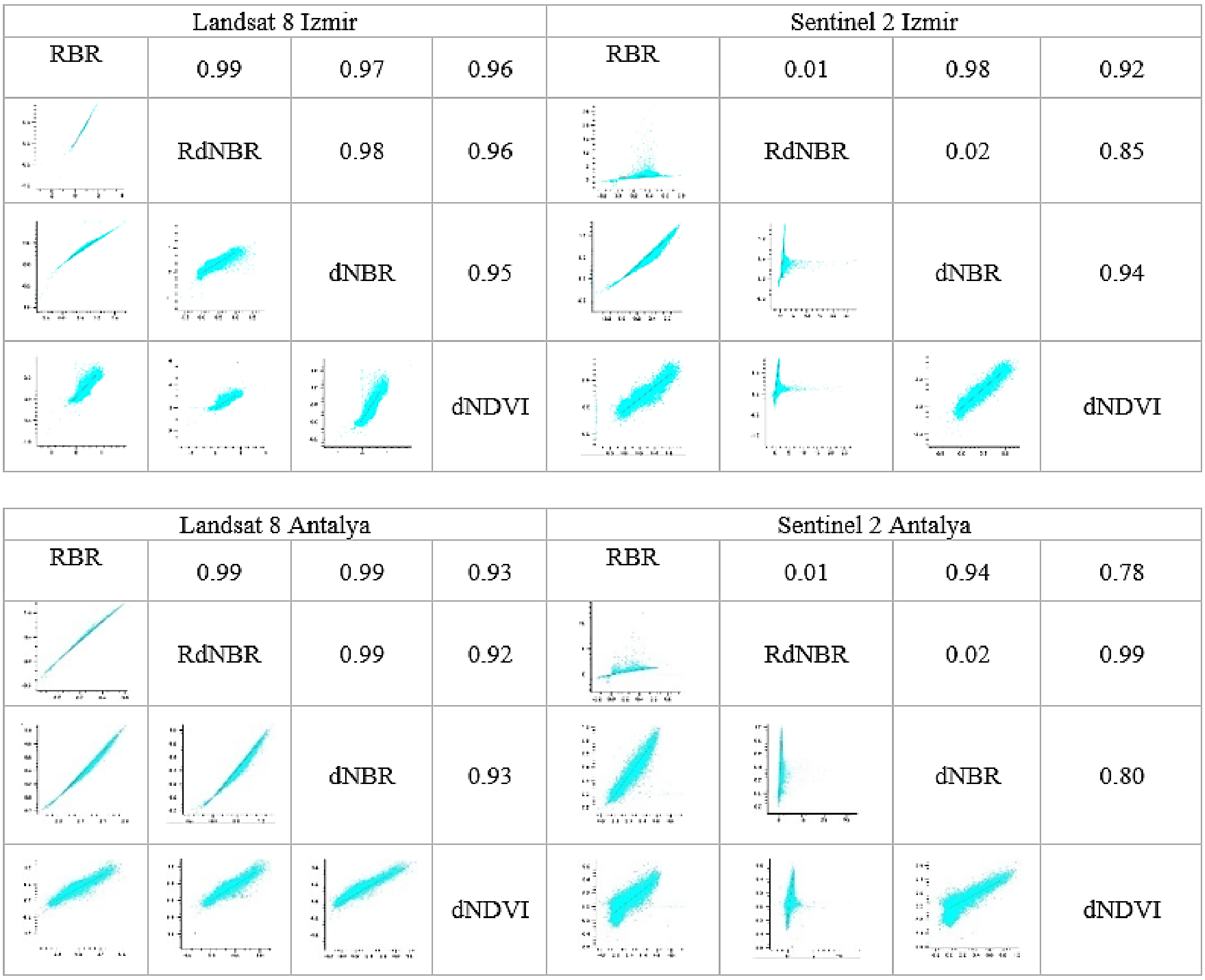

Fig. 6. The correlation graphs of fire severity indices produced from bi-temporal images

When the results are discussed, it can be asserted that burn severity indices that use SWIR bands provided a successful determination of burn scar; however, dNDVI faced some problems especially for the Sentinel 2 images. It is worth noting that, the index-based analysis results in different severity levels over burn scars. According to the burned area calculation results, it is observed that most of the index-based analysis tends to overestimate the total burned area when compared to image classification results.

The point-based accuracy metrics provided higher accuracies for index-based results from the Sentinel-2 image. Moreover, RdNBR provided the highest accuracies in both regions and for both sensors, which can be also verified from burn scar maps of this index provided in Figure 3. When the performance of ML classifiers is investigated, it can be observed that both SVM and RF classifiers provided similar and acceptable accuracies in terms of burned area mapping and overall classification performance. The burned area results are also comparable for these classifiers. On the other hand, these post-fire classification analyses can effectively map the burn scars, but cannot provide a quantitative result for burn severity levels.

Conclusion

The study investigated the performance of using moderate to high-resolution multispectral sensors such as Landsat 8 (OLI) and Sentinel 2 to evaluate burned forest area over two test sites. As a first step, we estimated the potential of four burn sensitive indices to ascertain the fire severity. Estimating the accuracy of binary classifications of these indices by employing active fire points from MODIS and VIIRS satellites represented that RdNBR assigned a higher percentage of accuracy over both satellite image sets in both study areas. Additionally, dNDVI provided higher burned area estimations for Landsat 8 images of both regions, whereas Sentinel 2 assigned RdNBR and dNBR for Karabağlar, Izmir, and Adrasan and Kumluca, Antalya respectively. Moreover, out of two widely used ML classifier algorithms, SVM and RF represented efficient performance in accuracy assessment for Adrasan and Kumluca, Antalya region. SVM classification of both satellite images provided relatively higher burned area. However, for Karabağlar, Izmir RF classification provided higher burned area estimations for Landsat 8 and Sentinel 2. The results conclude that RdNBR can be used as a reliable burn severity index and both machine learning-based classifiers can effectively map the burn scars.

Acknowledgements

Authors acknowledge the support of USGS and ESA by providing the Landsat 8 and Sentinel 2 satellite images free of charge.

References

Bar S, Parida BR, Pandey AC. (2020). Landsat-8 and Sentinel-2 based Forest fire burn area mapping using machine learning algorithms on GEE cloud platform over Uttarakhand, Western Himalaya. *Remote Sens Appl Soc Environ.*, 18, 100324.

Breiman L. (2001). Random forests. *Machine Learning*, 45, 5–32

Burak, S., Doğan, E., Gazioğlu, C. (2004). Impact of urbanization and tourism on coastal environment, *Ocean Coast Manag.*, 47, 15-527, 10.1016/j. ocecoaman.2004.07.007.

Chuvieco E, Martín MP, Palacios A. (2002). Assessment of different spectral indices in the red-near-infrared spectral domain for burned land discrimination. *Int J Remote Sens.*, 23(23), 5103–5110.

Collins L, Griffioen P, Newell G, Mellor A. (2018). The utility of Random Forests for wildfire severity mapping. *Remote Sens Environ.*, 216, 374–384.

Cutler DR, Edwards TC, Beard KH, Cutler A, Hess KT, Gibson J, Lawler JJ. (2007). Random forests for classification in ecology. *Ecology*, 88(11), 2783–2792.

Drusch M, Del Bello U, Carlier S, Colin O, Fernandez V, Gascon F, Hoersch B, Isola C, Laberinti P, Martimort P, et al. (2012). Sentinel-2: ESA's Optical High-Resolution Mission for GMES Operational Services. *Remote Sens Environ.*, 120, 25–36.

Erten E, Kurgun V, Musaoglu N (2004) Forest fire risk zone mapping from satellite imagery and GIS. a case study. *In: XXth international society for photogrammetry and remote sensing congress,* Istanbul, Turkey, 12–23 July 2004.

Evangelides C, Nobajas A. (2020). Red-Edge Normalised Difference Vegetation Index (NDVI705) from Sentinel-2 imagery to assess post-fire regeneration. *Remote Sens Appl Soc Environ.*, 17, 100283.

Fernández-García V, Santamarta M, Fernández-Manso A, Quintano C, Marcos E, Calvo L. (2018). Burn severity metrics in fire-prone pine ecosystems along a climatic gradient using Landsat imagery. *Remote Sens Environ.*, 206, 205–217.

Foody, G (2010). Assessing the accuracy of land cover change with imperfect ground reference data. *Remote Sens Environ*., 114, 2271-2285.

Fraser RH, Li Z, Cihlar J (2000). Hotspot and NDVI differencing synergy (HANDS): a new technique for burned area mapping over boreal forest. *Remote Sens Environ.*, 74, 362–376.

García-Llamas P, Suárez-Seoane S, Fernández-Guisuraga JM, Fernández-García V, Fernández-Manso A, Quintano C, Taboada A, Marcos E, Calvo L. (2019). Evaluation and comparison of Landsat 8, Sentinel-2 and Deimos-1 remote sensing indices for assessing burn severity in Mediterranean fire-prone ecosystems. *Int J Appl Earth Obs Geoinf.*, 80, 137–144.

Gibson R, Danaher T, Hehir W, Collins L. (2020). A remote sensing approach to mapping fire severity in south-eastern Australia using sentinel 2 and random forest. *Remote Sens Environ.*, 240, 111702.

Herrando S, Brotons L, Llacuna S. (2003). Does fire increase the spatial heterogeneity of bird communities in Mediterranean landscapes? *Ibis (Lond 1859)*, 145(2), 307–317.

Herrando S, Brotons L. (2002). Forest bird diversity in Mediterranean areas affected by wildfires: A multi-scale approach. *Ecography*, 25(2), 161–172.

Huang C, Davis L, Townshend J (2002). An assessment of support vector machines for land cover classification. *Int J. Rem. Sens.*, 23, 725-749

Huang H, Roy DP, Boschetti L, Zhang HK, Yan L, Kumar SS, Gomez-Dans J, Li J. (2016). Separability analysis of Sentinel-2A Multi-Spectral Instrument (MSI) data for burned area discrimination. *Remote Sens*, 8(10), 873.

Kesgin Atak B, Ersoy Tonyalıoglu E. (2020). Evaluating spectral indices for estimating burned areas in the case of Izmir / Turkey. *Eurasian J For Sci.* 8(1), 63–73.

Key C.H., and Benson, N.C. (2005). Landscape Assessment: Remote Sensing of Severity, the Normalized Burn Ratio and Ground Measure of Severity, the Composite Burn Index. FIREMON Fire Eff Monit Invent Syst USDA For Serv Rocky Mt Res.:Station 164.

Konkathi P, Shetty A. (2019). *Assessment of Burn Severity using Different Fire Indices: A Case Study of Bandipur National Park.* In Proc. IEEE Recent Adv Geosci Remote Sens Technol Stand Appl TENGARSS 2019, 151–154.

Laris PS. (2005). Spatiotemporal problems with detecting and mapping mosaic fire regimes with coarse-resolution satellite data in savanna environments. *Remote Sens Environ.*, 99(4), 412–424.

Louis J, Debaecker V, Pflug B, Main-Knorn M, Bieniarz J, Mueller-Wilm U, Cadau E, Gascon F. (2016). Sentinel-2 SEN2COR: L2A processor for users. Eur

Sp Agency, (Special Publ ESA SP. SP-740(May):9–13.

Lutes DC, Keane RE, Caratti JF, Key CH, Benson NC, Sutherland S, Gangi LJ. (2006). FIREMON: Fire effects monitoring and inventory system. Gen. Tech. Rep. USDA Forest Service RMRS-GTR-164-CD. (June):1–55.

Mallinis G, Mitsopoulos I, Chrysafi I. (2018). Evaluating and comparing sentinel 2A and landsat-8 operational land imager (OLI) spectral indices for estimating fire severity in a mediterranean pine ecosystem of Greece. *GIScience Remote Sens.*, 55(1), 1–18.

Miller JD, Knapp EE, Key CH, Skinner CN, Isbell CJ, Creasy RM, Sherlock JW (2009) Calibration and validation of the relative differenced Normalized Burn Ratio (RdNBR) to three measures of fire severity in the Sierra Nevada and Klamath Mountains, California, USA. *Remote Sens Environ*, 113, 645–656

Miller JD, Thode AE. (2007). Quantifying burn severity in a heterogeneous landscape with a relative version of the delta Normalized Burn Ratio (dNBR). *Remote Sens Environ.*, 109(1), 66–80.

Mouillot F, Schultz MG, Yue C, Cadule P, Tansey K, Ciais P, Chuvieco E. (2014). Ten years of global burned area products from spaceborne remote sensing-A review: Analysis of user needs and recommendations for future developments. *Int J Appl Earth Obs Geoinf*, 26(1), 64–79.

Navarro G, Caballero I, Silva G, Parra PC, Vázquez Á, Caldeira R. (2017). Evaluation of forest fire on Madeira Island using Sentinel-2A MSI imagery. *Int J Appl Earth Obs Geoinf.*, 58, 97–106.

Özcan, O.; Musaoglu, N.; Türkeş, M. (2018). Assessing vulnerability of a forest ecosystem to climate change and variability in the western Mediterranean sub-region of Turkey. *J. For. Res. 29*, 709–725.

Parks SA, Dillon GK, Miller C. (2014). A new metric for quantifying burn severity: The relativized burn ratio. *Remote Sens.*, 6(3), 1827–1844.

Rahman S, Chang HC, Magill C, Tomkins K, Hehir W. (2019). *Spatio-Temporal Assessment of Fire Severity and Vegetation Recovery Utilising Sentinel-2 Imagery in New South Wales, Australia*. Int Geosci Remote Sens Symp., 9960–9963.

Rodriguez-Galiano VF, Ghimire B, Rogan J, Chica-Olmo M, Rigol-Sanchez JP. (2012). An assessment of the effectiveness of a random forest classifier for land-cover classification. *ISPRS J Photogramm Remote Sens.*, 67(1), 93–104.

Roteta, E., Bastarrika, A., Padilla, M., Storm, T., Chuvieco, E., (2019). Development of a Sentinel-2 burned area algorithm: Generation of a small fire database for subSaharan Africa. *Remote Sens. Environ*. 222, 1–17

Roy DP, Wulder MA, Loveland TR, C.E. W, Allen RG, Anderson MC, Helder D, Irons JR, Johnson DM, Kennedy R, et al. (2014). Landsat-8: Science and product vision for terrestrial global change research. *Remote Sens Environ.,* 145, 154–172.

RTGDF. (2019). Forestry statistics, Republic of Turkey General Directorate of Forestry. Available online: https://www.ogm.gov.tr/tr/ormanlarimiz/resmi-istatistikler

Scholes RJ, Kendall J, Justice CO. (1996). The quantity of biomass burned in southern Africa. *J Geophys Res Atmos.*, 101(19), 23667–23676.

Seidl R, Thom D, Kautz M, Martin-Benito D, Peltoniemi M, Vacchiano G, Wild J, Ascoli D, Petr M, Honkaniemi J, et al. (2017). Forest disturbances under climate change. *Nat Clim Chang.,* 7(6), 395–402.

Sertel E, Alganci, U. (2016). Comparison of pixel and object-based classification for burned area mapping using SPOT-6 images. *Geomatics, Natural Hazards and Risk*, 7 (4), 1198-1206.

Shoko C, Mutanga O. (2017). Seasonal discrimination of C3 and C4 grasses functional types: An evaluation of the prospects of varying spectral configurations of new generation sensors. *Int J Appl Earth Obs Geoinf.*, 62, 47–55.

Silva JMN, Sá ACL, Pereira JMC. (2005). Comparison of burned area estimates derived from SPOT-VEGETATION and Landsat ETM+ data in Africa: Influence of spatial pattern and vegetation type. *Remote Sens Environ.*, 96(2), 188–201.

Sothe C, Almeida CMd, Liesenberg V, Schimalski MB. (2017). Evaluating Sentinel-2 and Landsat-8 Data to Map Sucessional Forest Stages in a Subtropical Forest in Southern Brazil. *Remote Sens*, 9(8), 838.

Soverel NO, Perrakis DDB, Coops NC. (2010). Estimating burn severity from Landsat dNBR and RdNBR indices across western Canada. *Remote Sens Environ.,* 114(9), 1896–1909.

Tran, BN, Tanase, MA, Bennett, LT, Aponte, C (2018). Evaluation of Spectral Indices for Assessing Fire Severity in Australian Temperate Forests. *Remote Sens.*, 10, 1680.

van der Werff H, van der Meer F. (2016). Sentinel-2A MSI and Landsat 8 OLI provide data continuity for geological remote sensing. *Remote Sens.*, 8(11), 883.

Zuhlke et al. 2015. SNAP (sentinel application platform) and the ESA sentinel 3 toolbox. [place unknown].